Magnetic Properties of $Sm(Co_{bal}Fe_{0.31}Zr_{0.05}Cu_{0.04}B_x)_z$ Alloys and Their Melt-Spun Materials $(x = 0.02–0.04, z = 7.5–12)$

M. Q. Huang, Z. Turgut, B. R. Smith, Z. M. Chen, B. M. Ma, S. Y. Chu, D. E. Laughlin, J. C. Horwath, and R. T. Fingers

***Abstract*—Cast alloys and melt-spun ribbons with nominal compositions of $Sm(Co_{bal}Fe_{0.31}Zr_{0.05}Cu_{0.04}B_x)_z$ $(x = 0.02–0.04, z = 7.5–12)$ have been synthesized and characterized in a temperature range of 10–1273 K and at fields up to 5T. The main phase in the as-cast alloys exhibited a Th_2Ni_{17} type structure, with a strong uniaxial anisotropy. Minor phases with a $TbCu_7$ and/or $CaCu_5$ structure emerged as z (3d/R) decreased. As a result, the anisotropy field (H_A) increased from 67 to 120 kOe, while $4\pi M_s$ fell from 12.8 to 10.5 kG at 300 K when z was decreased from 12 to 7.5. For melt-spun ribbons, they are nano-structured in nature and magnetically hard, even in the as-spun state. By lowering the value of z(3d/R) and raising the B content, a finer microstructure and a higher H_{ci} were obtained. Hard magnetic properties of $H_{ci} = 4.9–12$ kOe, $4\pi M_s = 9.0–12.0$ kG at 300 K have been obtained from ribbon samples. Among them, $Sm(Co_{bal}Fe_{0.31}Zr_{0.05}Cu_{0.04}B_{0.02})_{10}$ ribbon showed the highest $(BH)_{\max}$ of 10.8 MGOe at 300 K. A Henkel plot analysis suggested the existence of exchange-coupling interaction between the magnetically hard and soft phases in the ribbon materials.**

***Index Terms*—Exchange coupling, hard magnetic property, magnetic alloy, melt-spun, 3d/R.**

I. Introduction

NANOCOMPOSITE melt-spun Sm–Co-based materials have gained much attention in recent years because of their potential applications at elevated temperatures [1], [2]. A uniform and fine microstructure, strong anisotropic field, as well as high saturation magnetization are key factors for obtaining optimal magnetic performance. This can be achieved by alloy compositional adjustment and processing parameter optimization. Our previous work on the $Sm(Co_{bal}Fe_{1-x}Zr_{0.05}Cu_{0.08}Ga_yB_z)_{12}$ melt-spun alloys centered on the effect of Fe content on the magnetic properties [3]. $H_{ci} \sim 7$ kOe, $B_r \sim 6.95$ kG, and $(BH)_{\max} \sim 9.8$ MGOe at 300 K have been obtained from a melt-spun material with a Fe content of $x = 0.31$. In this study, we have extended our investigation to alloy system with a wider range of z (3d-transition metal/R-rare earth ratio) value from 7.5–12 to further enhance the magnetic properties. This work focuses on the effects of z and boron content on the phase formation, magnetic properties, and microstructure of both as-cast alloys and as-quenched melt-spun materials.

Manuscript received October 15, 2003. This work was supported in part by the Air Force Office of Scientific Research, Air Force Material Command.

M. Q. Huang and Z. Turgut are with UES Inc., Dayton, OH 45432 USA (e-mail: Meiqing.Huang@wpafb.af.mil; zturgut@ues.com).

B. R. Smith, Z. M. Chen, and B. M. Ma are with the Magnequench Technology Center, Research Triangle Park, NC 27709 USA (e-mail: Brsmith@mqii.com; Zhongmimchen@mqii.com; Baominma@mqii.com).

S. Y. Chu and D. E. Laughlin are with the Materials Science and Engineering Department, Carnegie Mellon University, Pittsburgh, PA 15213 USA (e-mail: sc79@andrew.cmu.edu; dl0p@andrew.cmu.edu).

J. C. Horwath and R. T. Fingers are with the Air Force Research Laboratory, Wright-Patterson Air Force Base, Dayton, OH 45433 USA (e-mail: john horwath@wpafb.af.mil; richard.fingers@wpafb.af.mil).

Digital Object Identifier 10.1109/TMAG.2004.828998

II. Experimental Detail

Cast alloy ingots with nominal compositions of $Sm(Co_{bal}Fe_{0.31}Zr_{0.05}Cu_{0.04}B_x)_z$ $(x = 0.02–0.04, z = 7.5–12)$ were prepared by arc melting under an Ar-atmosphere. The arc-melted ingot was further processed into melt-spun material. X-ray diffraction (XRD) with Cu radiation, and scanning electron microscopy (SEM and EDS) were used to determine the crystal structure, phases present and microstructure. Magnetic properties $(4\pi M_s, T_c, H_A$, and $H_{ci})$ were measured in the temperature range of 10–1473 K and at fields up to 5T, by using a vibrating sample magnetometer (VSM) and a superconducting quantum interference device (SQUID) magnetometer. Samples in the forms of chunk, loose, or aligned powder (<38 μm) were used for each prospective measurement. The anisotropy field (H_A) was estimated by measuring the easy and hard magnetization on powder aligned in a field of 2T and fixed in epoxy. Honda extrapolations were utilized to determine the saturation magnetization M_s. The exchange-interaction of the melt-spun samples was characterized via Henkel plots [4].

III. Results and Discussions

A. *$Sm(Co_{bal}Fe_{0.31}Zr_{0.05}Cu_{0.04}B_x)_z$ As-Cast Ingot Alloys*

Fig. 1(a) and (b) compares the XRD patterns of the random and magnetically aligned powder of $Sm(Co_{bal}Fe_{0.31}Zr_{0.05}Cu_{0.04}B_{0.02})_z$ cast ingots. As can be seen, the XRD patterns on the random powder samples indicate that the as-cast ingots consist of mixed phases. The structure and phases present vary systematically with the 3d/R ratio (z). For $z \leq 9$, the main phase exhibits a Th_2Ni_{17} (2:17) structure. However, it becomes a co-exist structure of Th_2Ni_{17} and Th_2Zn_{17} when $z < 9$. Minor phase with the $TbCu_7$ (1–7) or $CaCu_5$ (1–5) structure was detected and its amount was found to increase with decreasing z. A dilute (Co, Fe)-Zr phase is also detected via XRD and EDS. As seen in Fig. 1(b), the XRD patterns

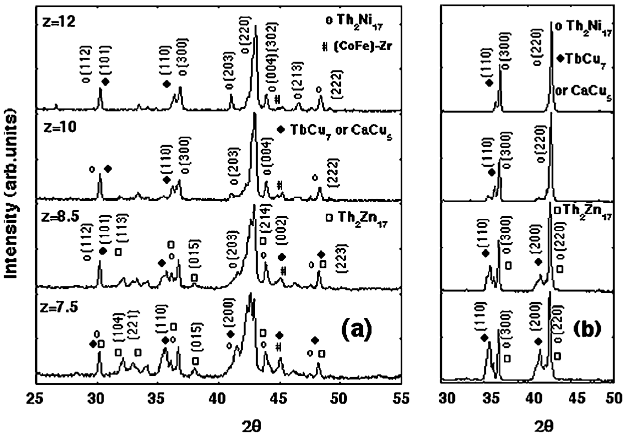

Fig. 1. XRD of $Sm(Co_{bal}Fe_{0.31}Zr_{0.05}Cu_{0.04}B_{0.02})z$ as-cast ingot alloys, measured on (a) random and (b) magnetically aligned powders.

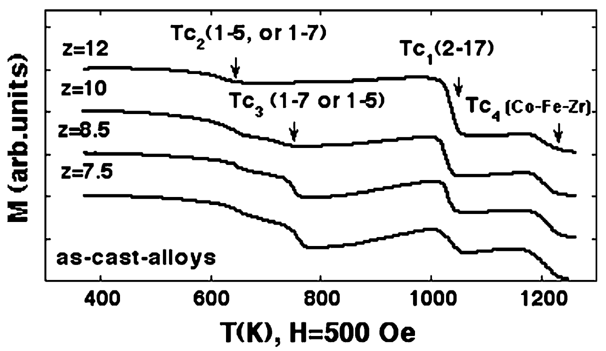

Fig. 2. M–T of $Sm(Co_{bal}Fe_{0.31}Zr_{0.05}Cu_{0.04}B_{0.02})_z$ as-cast ingot alloys measured at $H = 500$ Oe.

TABLE I
MAGNETIC PROPERTIES [$H_A, 4\pi M_s$, AND THEORETICAL $(BH)_{max}$] OF $Sm(Co_{bal}Fe_{0.31}Zr_{0.05}Cu_{0.04}B_x)_z$ CAST-ALLOYS AT 300 K AND 10 K

B	z(3d/R)	H_A (kOe) 300 K	H_A (kOe) 10 K	$4\pi M_s$ (kG) 300 K	$4\pi M_s$ (kG) 10 K	$(BH)_{max}$(MGOe) 300 K(theo)
0.02	7.5	120	155	10.5	11.2	27.5
0.02	8.0	103	155	10.9	11.4	29.6
0.02	8.5	94	152	10.8	11.7	29.2
0.02	9.0	88	148	11.9	12.8	35.6
0.02	10.0	82	136	12.2	13.6	37.4
0.02	12.0	67	102	12.8	13.8	41.2
0.04	8.0	92	149	10.6	11.3	28.3
0.04	10.0	84	125	11.5	12.1	33.0
0.04	12.0	71	102	12.5	12.9	39.1

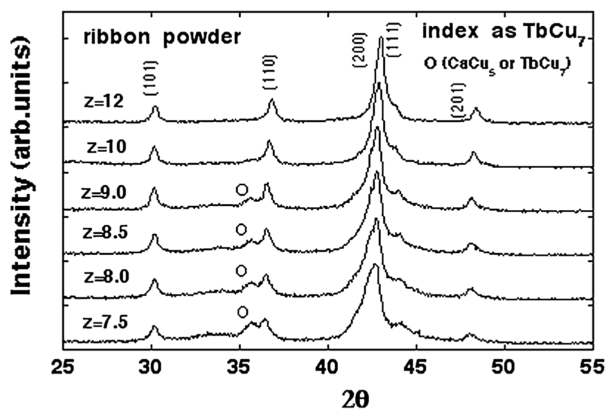

Fig. 3. XRD of $Sm(Co_{bal}Fe_{0.31}Zr_{0.05}Cu_{0.04}B_{0.02})_z$ as-quenched melt-spun alloys.

of the magnetically aligned powder samples indicate that all alloys present a strong uniaxial magnetocrystalline anisotropy. The two strengthened reflections can be indexed to the (300) and (220) of the Th_2Ni_{17} or Th_2Zn_{17} structure while the other two strengthened peaks can be indexed to the (110) and (200) reflections for the $TbCu_7$ or $CaCu_5$ structures. These results are also confirmed by the Curie temperature measurement.

Four Curie temperatures, denoted as Tc_1, Tc_2, Tc_3, and Tc_4 in Fig. 2, can be detected for $Sm(Co_{bal}Fe_{0.31}Zr_{0.05}Cu_{0.04}B_{0.02})_z$. They correspond to four types of magnetic phases: Tc_1 (1034–1045 K) for the (2–17) phase, Tc_2 (630–642 K) and Tc_3 (735–760 K) for the (1–5) and/or (1–7) phases, and Tc_4 (1217–1222 K) for the (Co, Fe)-Zr phase, respectively. It can be seen that the amount of (1–7) and/or (1–5) phases increases with decreasing z. The variation of anisotropy field, H_A, and saturation magnetization, $4\pi M_s$, with respect to the z ratios of $Sm(Co_{bal}Fe_{0.31}Zr_{0.05}Cu_{0.04}B_{0.02})_z$ as-cast alloys are listed in Table I. As expected, the H_A decreases while the $4\pi M_s$ increases with increasing z. This can be explained by the fact that the magnetocrystalline anisotropy of the (1–5) or (1–7) phase is higher than that of the (2–17) phase. The alloy with $z = 7.5$ possesses a high H_A (120 kOe), but low moment (10.5 kG) at 300 K. However, the alloy with $z = 12$ possesses a low H_A (67 kOe), but high $4\pi M_s$ (12.8 kG) at 300 K. Increasing the boron content from $x = 0.02$ to 0.04 was found to slightly enhance the H_A but at the cost of $4\pi M_s$ at 300 K for the alloys with z greater than 10. The theoretical $(BH)_{max}$ values of 27–41 MGOe at 300 K could be estimated using the experimental specific densities of 8.21–8.27 g/cm^3. These alloys exhibit potential for becoming exchange-spring magnets for elevated temperature applications if the proper microstructure can be developed.

B. As Quenched Melt-Spun $Sm(Co_{bal}Fe_{0.31}Zr_{0.05}Cu_{0.04}B_x)_z$

Similar to our previous work of $Sm(Co_{bal}Fe_{1-x}Zr_{0.05}Cu_{0.08}Ga_yB_z)_{12}$ melt-spun materials [3], the as-quenched melt-spun materials $Sm(Co_{bal}Fe_{0.31}Zr_{0.05}Cu_{0.04}B_x)_z$ have been found to exhibit nano-grained structure and can be indexed to the $TbCu_7$ type structures on their XRD patterns (shown in Fig. 3). It was noticed that the Th_2Ni_{17} structure may co-exist with the $TbCu_7$ structure. Because of the peak overlapping and line broadening, near the (203) reflection, it is difficult to index the reflections from the minor phase. With decreasing z, the hexagonal phase (1–7 or 1–5) can be detected and the widths of diffraction peaks become broad, suggesting a smaller grain size at lower z. A detailed microstructure investigation is to be reported by an accompanying paper [5]. The results indicated that the alloy with $z = 7.5$ comprises of nano-grains ($\sim$10 nm) in $TbCu_7$ type structure as the main phase. The main phase of alloy with higher z (12) is in the Th_2 Ni_{17} structure with nano-grain size at $\sim$50–80 nm. A soft magnetic phase (Co, Fe)$_{23}$ Zr_6 was detected as well. The microstructure of both free and wheel-contact surfaces of ribbons was also examined by XRD and SEM. As shown in Fig. 4, the nano-grains on the free surface exhibit

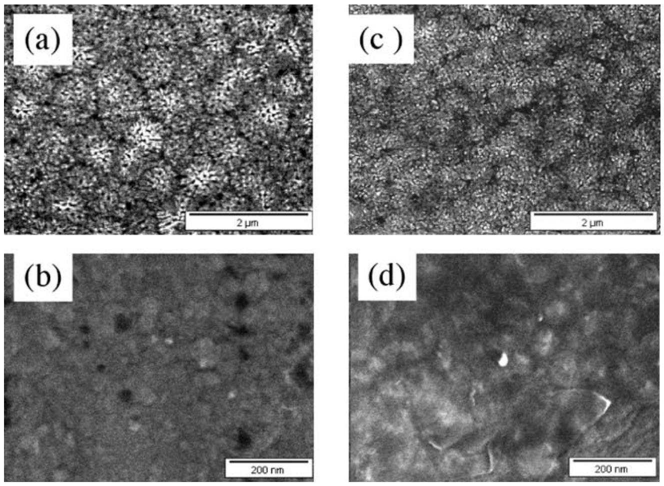

Fig. 4. SEM images of Sm($\mathrm{Co_{bal}Fe_{0.31}Zr_{0.05}Cu_{0.04}B_{0.02}}$)$_z$ as-quenched melt-spun alloys. (a), (d) on free surfaces of alloy ($z = 12$), (b) on wheel-contact surface of alloy ($z = 12$), (c) on free surface of alloy ($z = 9$).

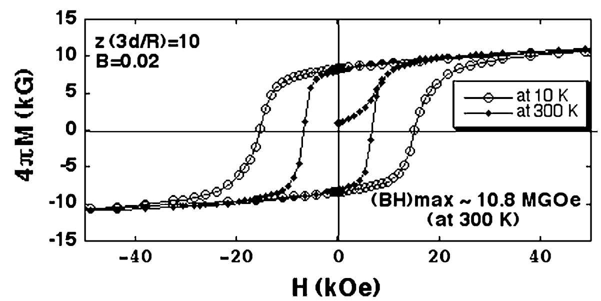

Fig. 5. $4\pi M$–H of Sm($\mathrm{Co_{bal}Fe_{0.31}Zr_{0.05}Cu_{0.04}B_{0.02}}$)$_{10}$ as-quenched melt-spun alloys.

cluster-like patterns, and they possess larger grain size than that on the wheel contact surface. The size of the clusters decreases with decreasing z and emerge into a more uniform microstructure. The fine and uniform grain size may contribute to the increase in H_{ci} observed on alloys of low z value.

Similar to the cast alloys, the hard magnetic properties of the melt-spun ribbons are also dictated by the intrinsic magnetic properties of the constituent phases and the microstructure. By lowering the z value, the coercivity H_{ci} at 300 K increases from 4.9 kOe for the alloy with $z = 12$ to 12 kOe of alloy with $z = 7.5$. As shown in Figs. 5 and 6, $H_{ci} = 4.9$–12 kOe, $4\pi M_s = 9.0$–12.0 kG, and $M_r/M_s \sim 0.67$ at 300 K and $H_{ci} = 10$–27 kOe at 10 K have been obtained in the melt-spun ribbon samples. As expected, when boron was increased from 0.02 to 0.04, the H_{ci} can be further increased but at the expense of $4\pi M_s$. It was also found that the optimal magnetic properties occur at $z \sim 10$ for this alloy system. The highest $(BH)_{\max}$ of 10.8 MGOe at 300 K has been observed on the ribbon with $z = 10$. As seen in Fig. 1, the initial magnetization curve indicated that as-spun ribbons exhibited a strong domain wall pinning behavior. Shown in Fig. 7 are the Henkel plots [δM–H] of three ribbons with $z = 7.5, 9$, and 12, respectively. The positive peaks of δM indicate the existence of exchange-coupling interaction between magnetically hard and

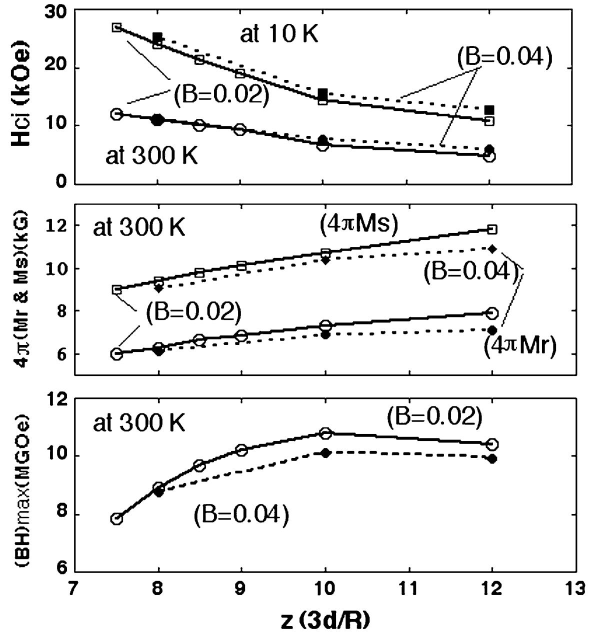

Fig. 6. Magnetic properties [$4\pi M_r, 4\pi M_s$, H_{ci}, and $(BH)_{\max}$] of Sm($\mathrm{Co_{bal}Fe_{0.31}Zr_{0.05}Cu_{0.08}B_x}$)$_z$ as-quenched melt-spun alloys ($x = 0.02$–$0.04, z = 7.5$–12) measured at 300 K and 10 K.

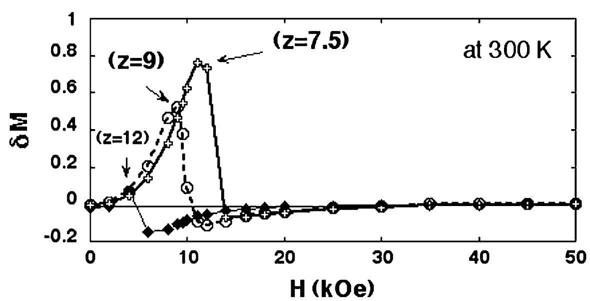

Fig. 7. Henkel plots [δM–H] of Sm($\mathrm{Co_{bal}Fe_{0.31}Zr_{0.05}Cu_{0.04}B_{0.02}}$)$_z$ as-quenched melt-spun alloys ($z = 7.5, 9$, and 12) at 300 K.

soft phases. The ribbon with lower z (7.5) exhibits a higher value of δM and a stronger exchange interaction could be partially contributed by exchange-coupling interaction between magnetically hard phases.

REFERENCES

[1] I. Panagiotopoulos, T. Matthias, D. Niarchos, and J. Fidler, "Magnetic properties and microstructure of melt-spun Sm(Co, Fe, Cu, Zr)8 magnets," *J. Magn. Magn. Mater.*, vol. 247, pp. 355–362, 2002.

[2] S. S. Markridis, G. Litsardakis, I. Panagiotopoulos, D. Nirachos, Y. Zhange, and G. C. Hadjipanayis, "High coercivity in boron substituted Sm-Co melt-spun magnets," *IEEE Trans. Magn.*, vol. 38, pp. 2922–2924, Sept. 2002.

[3] M. Q. Huang, Z. Turqut, B. R. Smith, Z. M. Chen, B. M. Ma, S. Y. Chu, J. C. Horwath, and R. T. Fingers, "Magnetic properties of Sm($\mathrm{Co_{bal}Fe_xZr_{0.05}Cu_{0.08}Ga_yB_z}$)$_{12}$ alloys and their melt-spun materials ($x = 0.1$–$0.4, y - 0 - 0.01, z = 0.01$–$0.02$)," *IEEE Trans. Magn.*, vol. 39, pp. 2902–2904, Sept. 2003.

[4] O. Hekel, "Weehselwrikungen in hartmagnetischen Teilchenko llektiven," *Phys. Stat. Sol.*, vol. 7, p. 919, 1964.

[5] R. Gopalan, D. H. Ping, K. Hono, B. Smith, Z. Chen, B. M. Ma, and M. Q. Huang, "Microstructure and magnetic properties of melt spun Sm($\mathrm{Co_{bal}Fe_xZr_{0.05}Cu_{0.08}Ga_yB_z}$)$_{12}$ alloys," presented at the 9th Joint 3M-Intermag Conf., Jan. 2004, Paper HG-06.